Ore Geology Reviews 46 (2012) 149–161

Contents lists available at SciVerse ScienceDirect

Ore Geology Reviews

journal homepage: www.elsevier.com/locate/oregeorev

Platinum-group elements in the oxide layers of the Hongge mafic–ultramafic intrusion, Emeishan Large Igneous Province, SW China

Zhong-Jie Bai [a,b], Hong Zhong [a,*], Chusi Li [c], Wei-Guang Zhu [a], Gui-Wen Xu [a,b]

[a] State Key Laboratory of Ore Deposit Geochemistry, Institute of Geochemistry, Chinese Academy of Sciences, Guiyang 550002, China
[b] Graduate University of Chinese Academy of Sciences, Beijing 100049, China
[c] Department of Geological Sciences, Indiana University, IN 47405, USA

ARTICLE INFO

Article history:
Received 28 July 2011
Received in revised form 9 February 2012
Accepted 9 February 2012
Available online 19 February 2012

Keywords:
Platinum-group elements
Layered intrusions
Magnetite layers
Sulfide segregations
Hongge intrusion
Emeishan Large Igneous Province

ABSTRACT

The Hongge layered intrusion (259.3 ± 1.3 Ma) is one of several mafic–ultramafic intrusions that host giant Fe–Ti–V oxide ore deposits in the ~260 Ma Emeishan Large Igneous Province (ELIP), SW China. The Hongge intrusion consists of a lower olivine clinopyroxenite zone (LOZ), a middle clinopyroxenite zone (MCZ) and an upper gabbro zone (UGZ). Most of the 14 to 84 m-thick and 300 to 1700 m-long economic Fe–Ti–V oxide ore layers occur within the MCZ. This paper reports the concentrations of PGE in the oxide layers of the Hongge intrusion. Unlike in the economic PGE (platinum-group elements) mineralized (up to 1.2 ppm Pt and 1.8 ppm Pd) coeval Xinjie intrusion (259 ± 3 Ma), the oxide layers in the Hongge intrusion contain very low PGE (total PGE: 0.09–63.5 ppb). Chromite-bearing horizons in the Hongge intrusion are enriched in IPGE (Ir: 0.46–0.65 ppb; Ru: 2.25–3.29 ppb) relative to PPGE (Pt: 0.54–1.28 ppb; Pd: 0.30–0.90 ppb). In contrast, the massive magnetite layers in the Hongge intrusion show no IPGE enrichments relative to PPGE. All our samples from the Hongge intrusion collectively show no correlation between PGE and S contents, and weak positive correlations between IPGE and Cr contents, indicating removal of Ir, Ru from magma with crystallization of chromite. Positive correlations exist between IPGE and PPGE in the samples, indicating that all of the PGE was controlled by sulfide liquid. Most of the samples have mantle-normalized PGE patterns with a slope similar to that of the Emeishan picritic basalts, which are less fractionated than the coeval high-Ti basalts derived from the same Fe-, Ti-, V-rich magma series. The Hongge oxide-rich samples are characterized by Cu/Pd ratios ($1.47–202 \times 10^4$) significantly higher than those for primitive mantle and the coeval picrites (0.99×10^4). The PGE tenors in bulk sulfides (i.e., in recalculated 100% sulfides) in the sulfide-bearing oxide ores of the Hongge intrusion (<0.1–3 ppm) are 2–3 orders of magnitude lower than the Xinjie intrusion (10–100 ppm). This, together with extremely high Cu/Pd ratios in both sulfide-bearing and sulfide-barren oxide-rich samples, indicates that the parental magma of the Hongge intrusion was depleted in PGE. We suggest that PGE depletion in the Hongge parental magma was due to previous sulfide segregation at depth, mainly due to crustal contamination. The PGE-depleted sulfides in the Hongge intrusion are thought to have formed by second-stage sulfide saturation and segregation due to fractional crystallization involving abundant magnetite after magma emplacement at Hongge.

1. Introduction

Two major types of magmatic ore deposits have been discovered in the mafic–ultramafic intrusions of the Emeishan large igneous province (ELIP); these are: 1. Cu–Ni–PGE sulfide deposits and PGE deposit in relatively small ultramafic bodies (e.g., Yangliuping, Jinbaoshan and Limahe; Song et al., 2003; Tao et al., 2007, 2008); and 2. Fe–Ti–V oxide deposits in larger mafic–ultramafic layered intrusions (e.g., Hongge, Panzhihua, Xinjie and Baima; Pang et al., 2008a,b, 2009; Zhong et al., 2002, 2003, 2004, 2011; Zhou et al., 2005). Sulfide and PGE enrichments in magnetite-bearing cumulates are present in many layered intrusions in the world, including the Rio Jacare intrusion in Brazil (Sa et al., 2005) and the Stella Intrusion in South Africa (Maier et al., 2003). In the ELIP, most PGE studies have focused on the sulfide-bearing intrusions and coeval basaltic rocks (Song et al., 2003, 2009; Tao et al., 2007; Zhong et al., 2006). However, a recent study on the Xinjie Fe–Ti–V oxide-bearing intrusion shows that some of the oxide layers in this intrusion, especially those with disseminated sulfides in the lower part of the intrusion, have very high PGE contents (up to 1.2 ppm Pt and 1.8 ppm Pd) (Zhong et al., 2011). This has prompted us to investigate the concentrations of PGE in the Fe–Ti oxide layers of the Hongge intrusion (~259.3 ± 1.3 Ma, Zhong and Zhu, 2006) which is coeval with the Xinjie intrusion (~259 ± 3 Ma, Zhou et al., 2002).

* Corresponding author. Tel.: +86 851 589 1820; fax: +86 851 589 1664.
E-mail address: zhonghong@vip.gyig.ac.cn (H. Zhong).

0169-1368/$ – see front matter © 2012 Elsevier B.V. All rights reserved.
doi:10.1016/j.oregeorev.2012.02.007

The Hongge intrusion hosts the largest magmatic Fe–Ti–V oxide deposit in the Panzhihua–Xichang (Pan–Xi) region. It contains 4572 Mt of oxide ores with 27 wt.% FeO, 10.6 wt.% TiO_2, and 0.24 wt.% V_2O_3 (Yao et al., 1993). The northern limb of the Hongge Fe–Ti–V deposit has been mined by the Longmang Company of China since 2003. Previous studies of PGE geochemistry and Sr–Nd isotope compositions were focused on the magma chamber processes and petrogenesis of the Hongge intrusion (Zhong et al., 2002, 2003). The current paper reports the results (total PGE: 0.09–63.5 ppb) of more complete PGE analyses for all of the important Fe–Ti oxide-rich layers in the intrusion. In the paper we use our new data to evaluate the economic potential of PGE in the Fe–Ti oxide layers of the intrusion as well as sulfide saturation history and PGE fractionation processes during the crystallization of the intrusion.

2. Geological background

The Pan–Xi area is located in the western margin of the Yangtze block, to the east of the Tibetan plateau. The basement of the Yangtze block comprises the Paleo-Mesoproterozoic Huili Group or its equivalents, the Yanbian and Kunyang Groups, which consist of low-grade metasedimentary rocks interbedded with felsic and mafic metavolcanic rocks, and the Neoproterozoic Kangding Complex, composed of granulite–amphibolite facies metamorphic rocks. The western margin of the Yangtze block is marked by abundant Neoproterozoic igneous rocks, consisting dominantly of mid-Neoproterozoic (830–740 Ma) felsic intrusive and volcanic rocks, and minor mafic/ultramafic rocks, including basaltic lavas, sills, dikes and small intrusions (e.g., Li et al., 2003, 2006; Zhou et al., 2006; Zhu et al., 2006).

The geology of the ELIP (Fig. 1) has been described in detailed in previous studies (e.g., Chung and Jahn, 1995; Xiao et al., 2004a; Xu et al., 2001, 2007; Zhang et al., 2006, 2008, 2009). The ELIP is composed of massive flood basalts, numerous mafic–ultramafic layered intrusions, granites, syenites and other alkaline intrusions, covering a large part of SW China (Zhang et al., 2008; Zhu et al., 2010). The late Permian Emeishan continental flood basalts (ECFB), overlying the late Permian limestone of the Maokou formation, are exposed in the western Yangtze block over more than 5×10^5 km^2 (Xiao et al., 2004a,b). The thickness of the basaltic sequence varies from several hundred meters in the east part of the province to over 5000 m in the west part of the province (Xu et al., 2001). The ECFB mainly consists of tholeiitic basalt, with minor picritic basalt, alkaline basalt and rhyolitic/trachytic flows, and has been divided into high-Ti ($TiO_2>2.5$ wt.%, Ti/Y > 500) group distributed across almost the entire province and low-Ti ($TiO_2<2.5$ wt.%, Ti/Y < 500) group exposed only in the southwest part of the province (Xiao et al., 2004a; Xu et al., 2001).

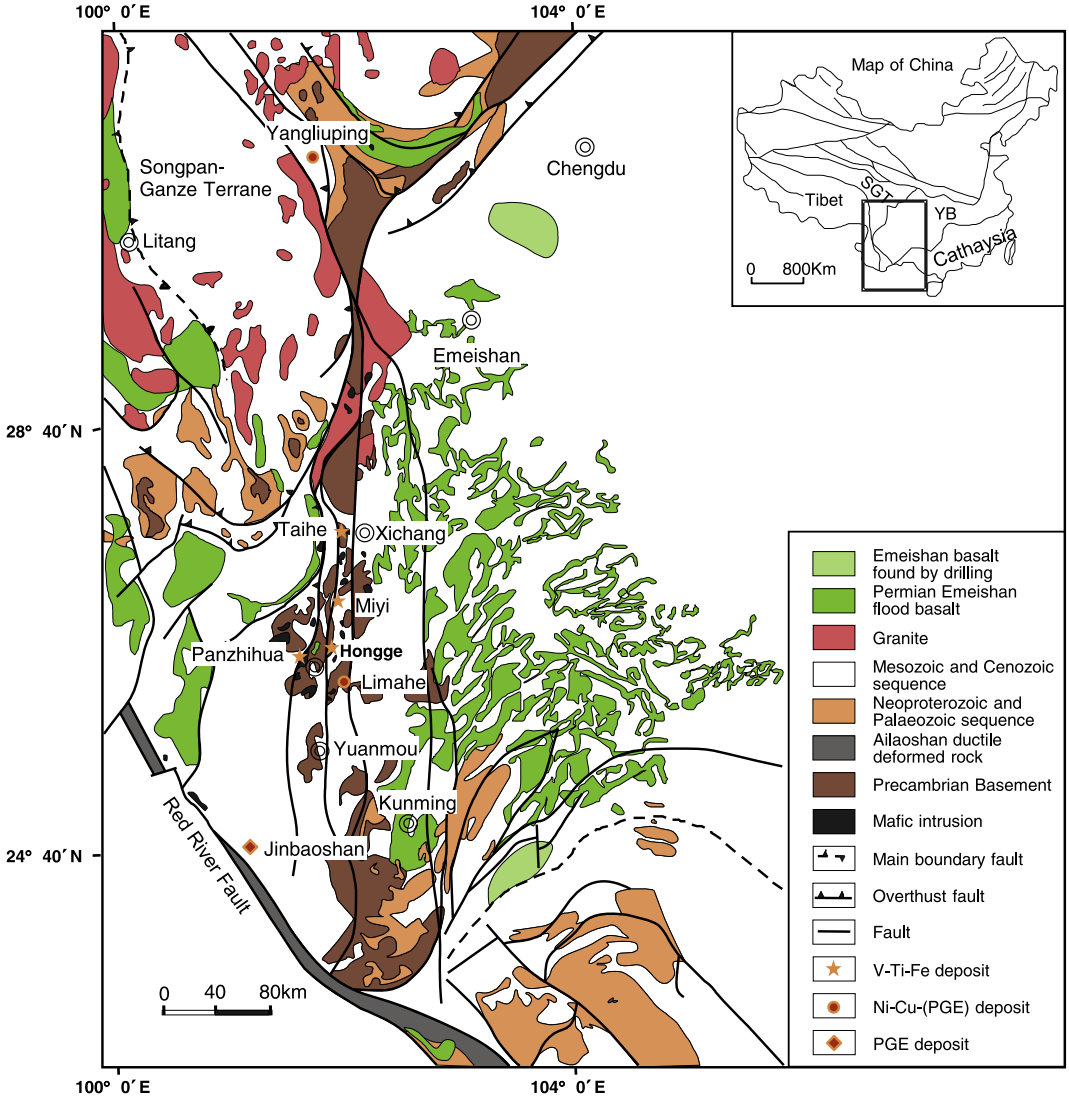

Fig. 1. Distribution of continental flood basalts and contemporaneous mafic–ultramafic intrusions, the Emeishan large igneous province, South China (modified from Zhou et al., 2002). SGT = Songpan–Ganze Terrane; YB = Yangtze Block.

Numerous mafic–ultramafic layered intrusions containing Fe–Ti oxide deposits and Cu–Ni–(PGE) sulfide mineralization are exposed in the Pan–Xi area that has been affected by several major north–south-trending faults. These intrusions, including the Hongge, Xinjie, and Limahe mafic–ultramafic intrusions and the Panzhihua, Baima and Taihe mafic intrusions, form a 200-km-long intrusive belt. Recently, zircon U–Pb dating results reveal that the mafic–ultramafic intrusions were emplaced at ~260 Ma (Guo et al., 2004; Zhong and Zhu, 2006; Zhou et al., 2002, 2005, 2008). The small sill-like intrusive bodies (e.g., Jinbaoshan, Tao et al., 2007; Baimazhai, Wang and Zhou, 2006; Wang et al., 2006; Yangliuping, Song et al., 2003) contain magmatic Cu–Ni–(PGE)-bearing sulfide deposits. These intrusions mainly consist of peridotites, websterite, olivine pyroxenite, pyroxenite and gabbro. Their parental magmas are probably related to the low-Ti basalts of the ELIP (e.g., Jinbaoshan; Tao et al., 2007; Zhou et al., 2008). In contrast, the large layered intrusions containing Fe–Ti oxide deposits are thought to be related to the high-Ti basalts of the ELIP (e.g., Hongge, Xinjie, Baima and Panzhihua; Wang et al., 2008; Zhong et al., 2002, 2003, 2004; Zhou et al., 2005, 2008). A modeling by MELTS program (Ghiorso and Sack, 1995) indicates that the parental ferrobasaltic magma of the Hongge intrusion has about 14.5 wt.% FeO, 3.51 wt.% TiO_2 and 385 ppm V, which experienced ~22% crystallization from the primitive Emeishan picritic magma. Multiple pulses of such Fe-, Ti-, V-rich basaltic magma were involved in the formation of the Hongge intrusion and related Fe–Ti–V oxide deposit in a magma stepwise flow-through system (Bai et al., in press).

3. Geology and petrography of the Hongge layered intrusion

The 16 km-long, 3–6 km-wide and 1.2 km-thick Hongge layered intrusion (Fig. 2) intruded the dolomitic limestones of the Neoproterozoic Dengying formation and the granitic gneisses of the Neoproterozoic Kangding Complex. The Dengying Formation in contact with the intrusion has been metamorphosed to marbles. The Hongge intrusion contains greenschist-facies metamorphosed basaltic xenoliths. Part of the intrusion at the northeast corner is overlain by ~180 m-thick basaltic sequence of the ECFB. The north and west contact zones of the intrusion were intruded by the late Permian alkaline granites and alkaline syenites. The results of precise zircon U–Pb age dating indicate that the Hongge intrusion crystallized at ~259.3 ± 1.3 Ma (Zhong and Zhu, 2006). The strongly differentiated Hongge intrusion is dominated by clinopyroxenites, olivine clinopyroxenites and gabbros, and has been divided into three lithological zones based on the appearance or disappearance of cumulus minerals from the base to the top: the lower olivine clinopyroxenite zone (LOZ), the middle clinopyroxenite zone (MCZ), and the upper gabbro zone (UGZ) (Figs. 2 and 3; Zhong et al., 2002). The LOZ and MCZ are marked by the appearance and disappearance of olivine whereas the UGZ is marked by the appearance of abundant euhedral apatite. The MCZ was further divided into two subzones: upper MCZ (UMCZ) and lower MCZ (LMCZ) (Fig. 2; Zhong et al., 2002).The massive Fe–Ti oxide bodies mainly occur in the lower and middle part of the UMCZ and LMCZ (Fig. 3) as layers with different thickness and gradational contacts with the host rocks. Samples containing >50 modal% of Fe–Ti oxide (magnetite + ilmenite) are termed massive oxides in this study.

The LOZ is about 340 m in thickness. It is composed of dark, medium- to fine-grained rocks containing clinopyroxene, magnetite and ilmenite, with minor olivine, chromite, hornblende and plagioclase. Euhedral to subeuhedral olivine is enclosed in subeuhedral to anhedral cilnopyroxene crystals. Fine-grained magnetite and ilmenite mainly occur in the interstitial spaces between olivine and clinopyroxene. In

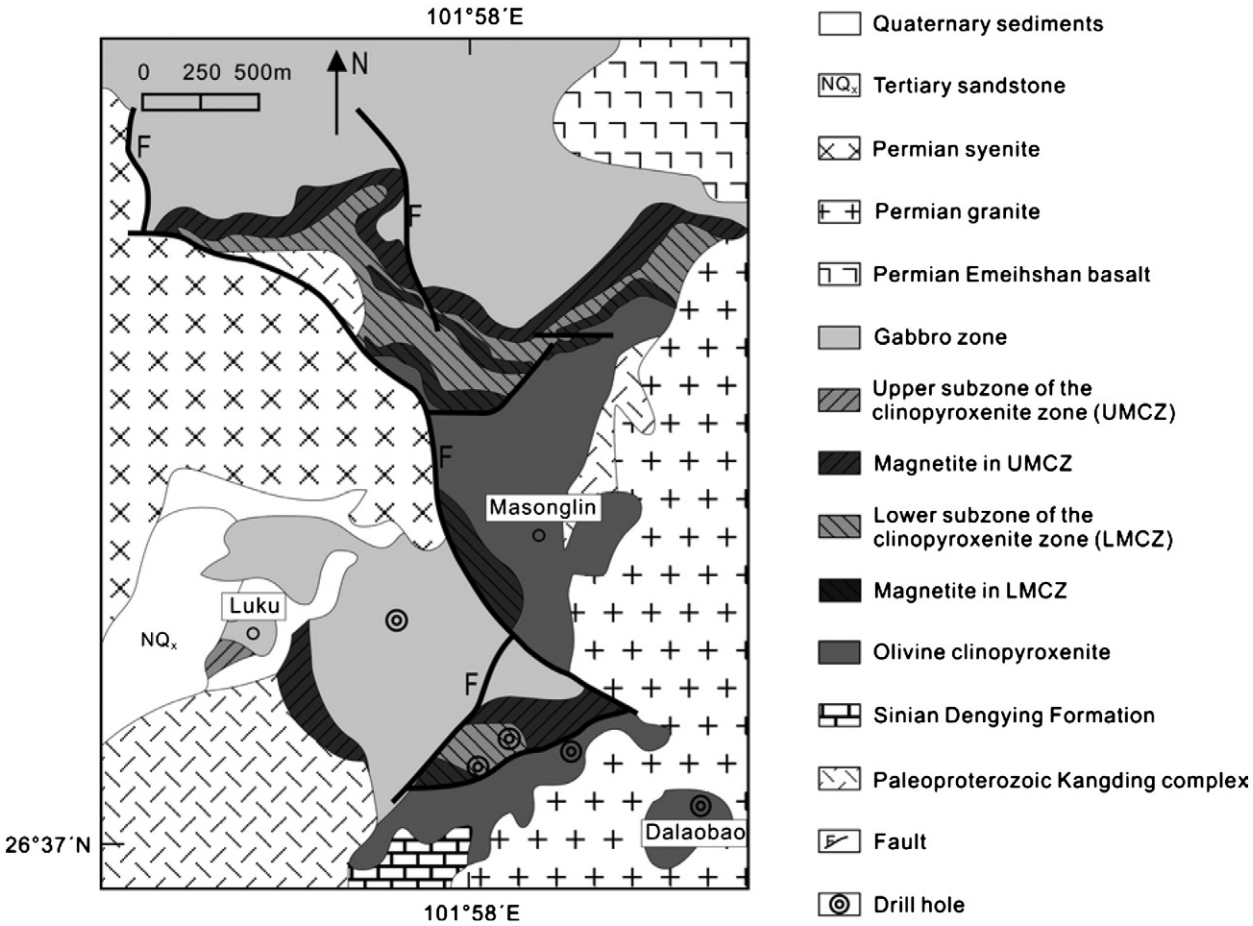

Fig. 2. Simplified geological map of the Hongge layered intrusion (modified from Yao et al., 1993). The lithological units are the same as in Fig. 3.

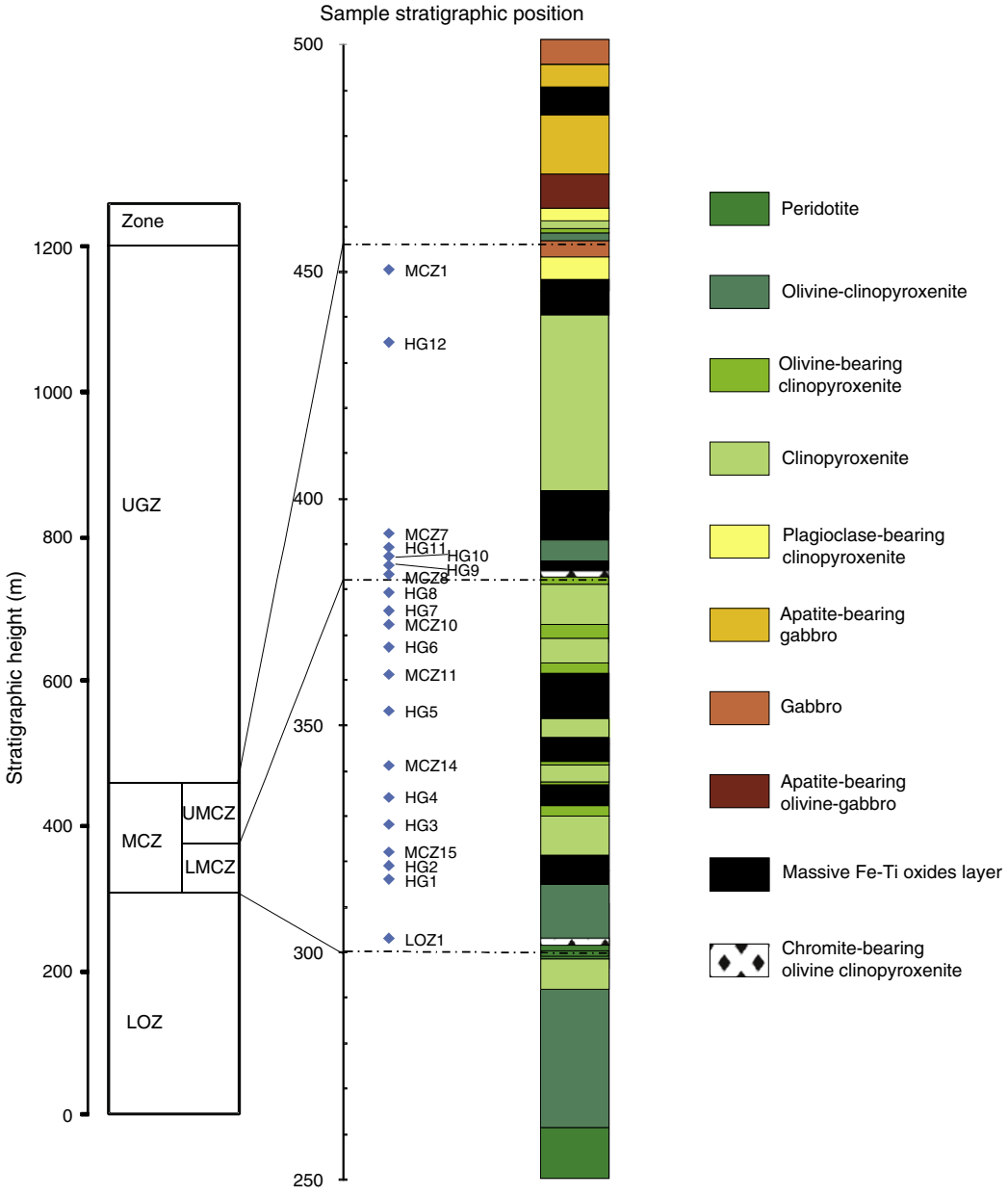

Fig. 3. Stratigraphic distribution of rock units in the Hongge intrusion, with sample locations.

some samples magnetite and ilmenite are also present as small inclusions in olivine and clinopyroxene crystals. Minor amounts of olivine and Cr-spinel occur in the rocks beneath the massive Fe–Ti oxide layers. The abundance of plagioclase increases progressively from the base to the top in the UMCZ and LMCZ. Some clinopyroxene crystals in the base of the MCZ contain exsolved Fe–Ti oxides. The MCZ hosts the major Fe–Ti–V oxide layers. The UGZ is about 780 m thick and consists of plagioclase, clinopyroxene, with minor olivine in its base. Euhedral apatite, commonly occurs as inclusions in olivine and plagioclase, is most abundant in the lower part of the UGZ.

The MCZ and UGZ host massive to disseminated V- and Ti-rich magnetite layers with thickness and length vary from 14 to 84 m and from 300 to 1700 m, respectively. The oxide layers in the MCZ are most important economically (PXGT, 1987; Yao et al., 1993; Zhong et al., 2002). These layers also contain elevated Ni (~0.10 wt.%), Co (~0.02 wt.%) and Cu (~0.04 wt.%) due to the presence of 0.5–3.5% disseminated sulfides (PXGT, 1987). The sulfide textures include: (1) intercumulus assemblages between oxide and silicate minerals; (2) rounded inclusions within Fe–Ti oxide crystals; (3) stringers or veinlets. Pyrrhotite is the major sulfide mineral, accounting for ~90% of the sulfide assemblages. Other minor sulfides include pentlandite, pyrite, chalcopyrite, and cubanite. Sperrylite, vincentite and laurite are the most common platinum-group minerals (PGM) associated with base metal sulfides in the intrusion (Liang et al., 1998).

4. Sampling and analytical methods

The samples analyzed in this study are from the MCZ of the Hongge intrusion except the picrite sample (DJ0805) collected from the Lijiang area. Eight samples (LOZ*–MCZ*) used in this study were collected from four drill cores (CK190, CK796, CK810, and CK802) located within the Hongge intrusion, and the other twelve samples (HG01–HG12) were collected from the surface of the intrusion. The stratigraphic positions of these samples are shown in Fig. 3.

Table 1
PGE (ppb), Cr, Ni, Cu (ppm) and S (wt.%) concentrations of the Hongge layered intrusion.

Sample no.	DJ0805	LOZ1	HG01	HG02	MCZ15	HG03	HG04	MCZ14	HG05	MCZ11	HG06	MCZ10	HG07	HG08	MCZ28	HG09	HG10	HG11	MCZ27	HG12	MCZ1
Rock type	Picrite	Ocp	Ore	Ore	Cp	Cp	Ore	Cp	Ore	Ore	Cp	Ocp	Ore	Cp	Ocp	Ocp	Ocp	Ocp	Ocp	Cp	Ore
Height (m)	–	303	316	319	322	328	334	341	353	361	367	372	375	379	383	385	387	389	392	434	450
Ir	1.80	0.115	3.74	0.009	0.101	0.003	0.026	0.208	0.052	0.058	0.14	0.27	0.031	0.002	0.77	0.65	1.87	0.46	0.62	0.46	0.63
Ru	3.17	0.184	8.10	0.020	0.159	0.007	0.042	0.106	0.040	0.114	0.31	0.50	0.040	0.005	1.11	3.29	6.80	0.76	0.88	2.25	0.98
Rh	0.68	0.060	1.99	0.006	0.076	0.002	0.024	0.072	0.014	0.092	0.067	0.08	0.015	0.000	0.21	0.41	1.78	0.17	0.25	0.13	0.23
Pt	11.6	1.33	27.0	0.21	1.48	0.036	0.32	1.46	0.62	2.42	0.67	2.09	0.45	0.043	3.50	0.54	25.2	2.19	5.19	1.28	4.66
Pd	9.77	0.84	22.7	0.20	10.0	0.101	0.35	0.75	0.26	2.00	0.39	0.89	0.48	0.045	2.08	0.30	18.1	1.57	2.08	0.90	2.05
PGE	27.0	2.53	63.5	0.45	11.8	0.15	0.76	2.60	0.99	4.68	1.58	3.85	1.01	0.09	7.67	5.19	53.7	5.15	9.02	5.02	8.56
Ni[a]	935	540	823	347	318	64.9	732	332	868	837	367	293	880	15.4	781	895	994	794	543	431	153
Cu[a]	96.4	119	334	411	183	42.1	241	286	462	406	74.1	37	479	78.6	67	151	449	328	338	64.5	77
Cr[a]	–	1239	8630	32.5	1398	577	148	1463	221	532	3110	1573	210	10.8	1426	5200	7960	1630	2878	2570	188
S	–	0.25	0.03	0.32	0.26	0.01	0.34	0.67	0.43	0.54	0.03	0.12	0.45	0.40	0.05	0.20	0.35	0.50	0.66	0.39	0.75
Pd/Ir	5.44	7.33	6.06	22.6	99.5	38.1	13.6	3.60	5.04	34.4	2.76	3.31	15.5	25.2	2.71	0.45	9.68	3.41	3.33	1.95	3.25
Pt/Ir	6.46	11.6	7.24	23.3	14.7	13.5	12.3	7.03	12.0	41.6	4.70	7.74	14.5	24.2	4.54	0.82	13.5	4.75	8.33	2.77	7.37
Pt/Pd	1.19	1.59	1.19	1.03	0.15	0.35	0.90	1.96	2.37	1.21	1.70	2.34	0.94	0.96	1.68	1.81	1.39	1.39	2.50	1.42	2.27
Cu/(Pd×10^4)	0.99	14.16	1.47	202.67	1.83	41.61	68.87	38.2	176	20.3	18.9	4.14	101	176	3.21	51.0	2.48	20.8	16.3	7.17	3.75

Note: Ocp — olivine clinopyroxenite; Cp — clinopyroxenite.
[a] The data of Ni, Cu, Cr are from Bai et al. (in press).

Platinum-group elements were determined by isotope dilution (ID)-ICP-MS using an improved Carius tube technique (Qi et al., 2007). The mono-isotope element Rh was measured by external calibration using a ^{194}Pt spike as internal standard (Qi et al., 2004). Eight grams of rock powder and appropriate amount of enriched isotope spike solution containing ^{193}Ir, ^{101}Ru, ^{194}Pt, and ^{105}Pd were digested using ~27 ml aqua regia in a 75 ml Carius tube placed in a sealed, custom-made, high pressure, water-filled autoclave (Qi et al., 2007). The total procedural blanks were lower than 0.002 ppb for Ir and Rh; 0.012 ppb for Ru; 0.040 ppb for Pd; and 0.002 ppb for Pt. As shown in Supplementary data 1, the results of the standard reference material WGB-1 (gabbro) agree well with the values reported by Qi et al. (2008). The accuracies are estimated to be better than 10% for all PGEs. Sulfur contents were determined by a C–S analyzer at the SKLODG, Institute of Geochemistry, Chinese Academy of Sciences.

5. Analytical results

The concentrations and variations of PGE and S in the studied samples are listed in Table 1 and Fig. 4. The contents of S in the samples vary from ~0.02 wt.% to 0.8 wt.% and tend to be higher in the massive magnetite layers than in the host rocks (Fig. 4a, b). The concentrations of Cr are highest at the bases of the LMCZ and UMCZ and decrease upward in these two zones from 8630 to 10 ppm and 5200 to 188 ppm, respectively. The contents of Ni and Cu in these two zones vary between 15 and 993 ppm, and between 37 and 479 ppm, respectively (Fig. 4c, d, e; Bai et al., in press). The contents of PGE in all the samples analyzed are very low and highly variable, with total PGE ranging from 0.09 to 63.5 ppb (Fig. 4f). Samples with higher PGE contents tend to occur in the lower part of the LMCZ (27.1 ppb Pt, 22.7 ppb Pd, 3.74 ppb Ir, 8.10 ppb Ru, 1.99 ppb Rh) or the lower part of the UMCZ (25.2 ppb Pt, 18.1 ppb Pd, 1.87 ppb Ir, 6.81 ppb Ru, 1.78 ppb Rh) (Fig. 4g–j). Except for two samples from the bases of the LMCZ and UMCZ, all other samples have PGE concentrations (0.036–5.19 ppb Pt, 0.045–10 ppb Pb) much lower than that of the coeval picrites in the region (Table 1). The abundances of PGE in the massive magnetite layers and associated rocks of the Hongge intrusion are in the same range. The Pt/Pd ratios of all the samples vary from 0.15 to 2.5, mostly from 0.94 to 2.5. Platinum is slightly higher than Pd in most samples, except for samples MCZ15 and HG03 which contain Pd one order of magnitude higher than Pt. The Pt/Ir and Pd/Ir ratios (Fig. 4k) of all the samples range from 0.45 to 99.5 and from 0.83 to 40.3, respectively, and show no clear correlation with magnetite abundance (Table 1). The Cu/Pd ratios of all the samples are highly variable (1.47×10^4–2.02×10^6) and appear to show a broadly negatively correlated with total PGE abundance (Fig. 4l).

The primitive mantle-normalized PGE patterns of each sample are similar except two chromites-bearing samples (e.g., HG09 and HG12) which show IPGE enrichments relative to PPGE (Fig. 5). Two samples (MCZ14 and HG05) are depleted in Ru relative to Ir and Rh whereas all other samples are significantly depleted in PGE compared to primitive mantle.

6. Discussion

6.1. Controls on PGE distribution and fractionation

All the samples from the MCZ used in this study contain very low (0.09–63.5 ppb) but variable total PGE contents (Table 1). The primitive mantle normalized patterns of PGE in the samples from the MCZ of the Hongge intrusion are characterized by positive slopes except the chromite-bearing samples (e.g., HG09 and HG12) (Fig. 5). The PGE patterns for the chromite-bearing samples are characterized by negative slopes, reflecting IPGE (Os, Ir, Ru) enrichments relative to PPGE (Pt, Pd). It is well known that the distribution of PGE in mafic and ultramafic rocks is most commonly controlled by sulfides,

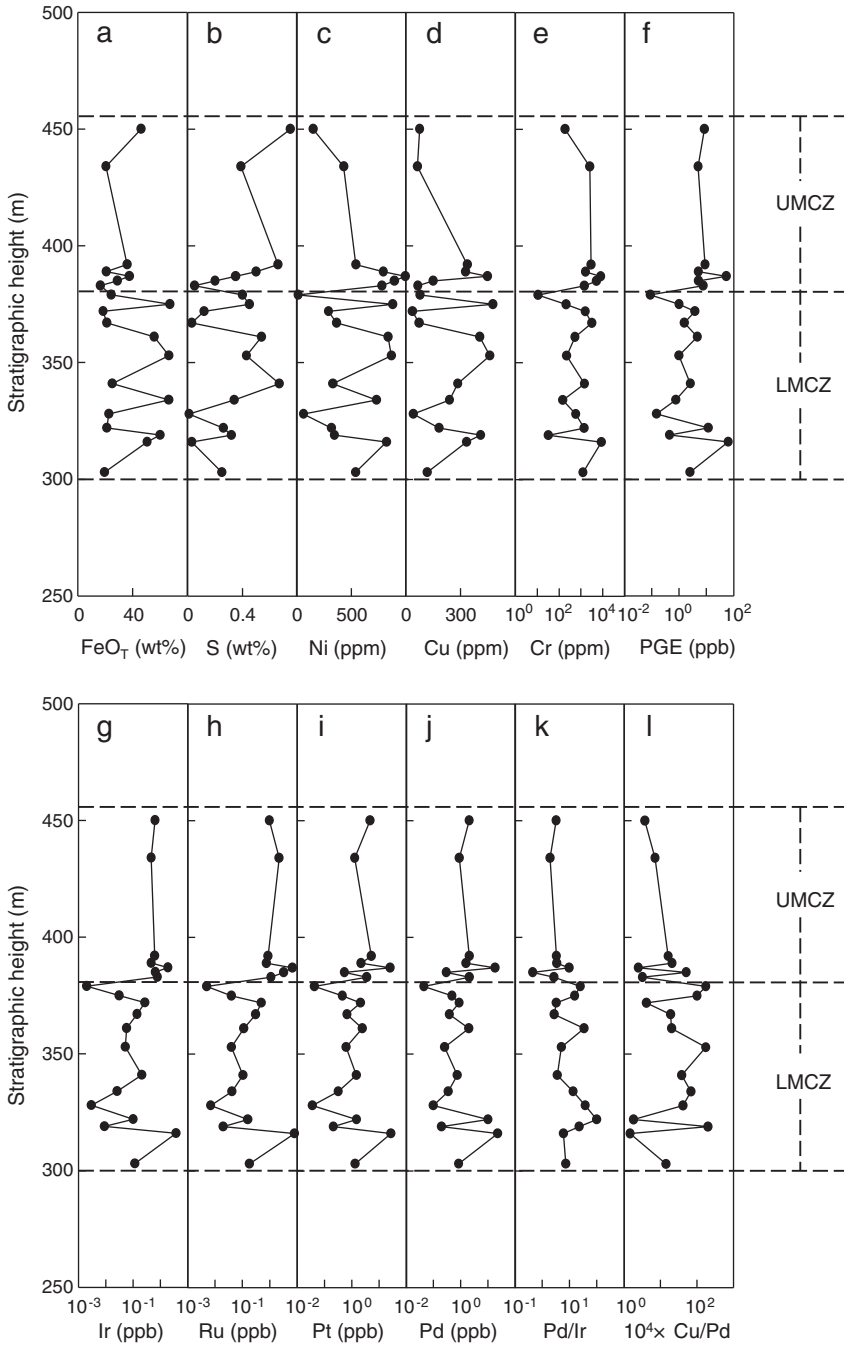

Fig. 4. Stratigraphic variations of FeO$_T$, S, Ni, Cu, Cr, $10^4 \times$Cu/Pd, Ir, Ru, Pt, Pd, PGE, and Pd/Ir in the Hongge intrusion. FeO$_T$, Ni, Cu, and Cr contents are from Bai et al. (in press).

chromite, olivine and PGMs (e.g., Barnes et al., 1985). Experimental results and theoretical calculations indicate that IPGE are more compatible than PPGE in chromite and olivine and may fractionate from each other during fractional crystallization of these minerals from magma (Barnes and Picard, 1993; Brenan et al., 2003, 2005, 2012; Peach and Mathez, 1996; Puchtel and Humayun, 2001; Righter et al., 2004). The occurrence of magmatic cumulus IPGE-rich phases as inclusions or "micro-nuggets" enclosed within olivine and chromite may also play an important role in PGE fractionation (Ballhaus and Sylvester, 2000; Ballhaus et al., 2006; Keays, 1982; Locmelis et al., 2011; Maier and Barnes, 1999; Melcher et al., 1997; Pagé et al., 2012; Sattari et al., 2002). The positive anomalies of IPGE in the chromite-bearing samples HG09 and HG12 and negative anomalies in the chromite-barren samples HG04 and MCZ14 (Fig. 5), as well as the positive correlation between Cr and Ir and Ru (Fig. 6), suggest removal of Ir, Ru from magma either as solid solution in Cr-spinel structure or as IPGM inclusions enclosed within chromite during the early stages of magma evolution at Hongge.

Chalcophile elements such as Ni, Cu and PGE strongly partition into sulfide liquid due to their high partition coefficients between sulfide liquid and silicate melt (10^4–10^5 for PGE: Bezmen et al., 1994; Crocket et al., 1997; Fleet et al., 1996; Peach et al., 1994; Stone et al., 1990 or ~10^7–10^{11} for PGE, Fonseca et al., 2009. 10^2–10^3 for Cu and Ni: Francis, 1990; Gaetani and Grove, 1997; Peach et al., 1990; Rajamani and Naldrett, 1978). The weak correlations between S, Cu and PGE in the Hongge samples (Fig. 7) indicate that sulfide liquid was not the only collector of PGE or that the sulfide liquids involved had highly variable Cu and PGE concentrations. Alternatively, this may be due to the occurrence of discrete PGM independent of the sulfide content of the rock. Such discrete PGM can be either primary (i.e.,

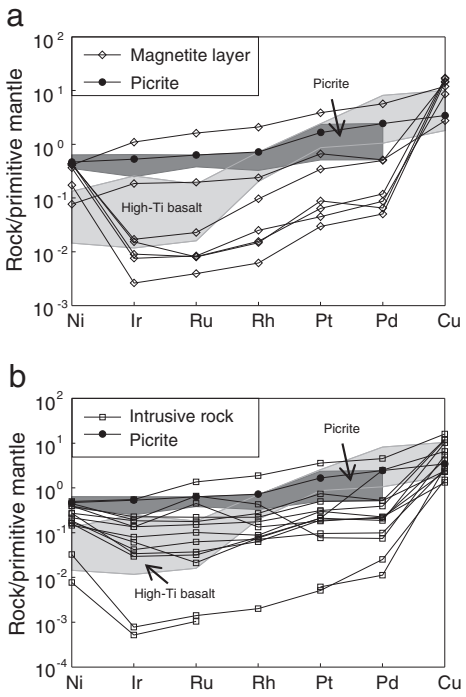

Fig. 5. Primitive mantle-normalized chalcophile element patterns of massive magnetite layers (a) and silicate rocks (b) in the Hongge intrusion. The primitive mantle values are from Barnes and Maier (1999). The values for the Emeishan high-Ti basalts are from Zhong et al. (2006) and Song et al. (2009); the values for the Emeishan picrites from Zhang et al. (2005) and Zhong et al. (2006).

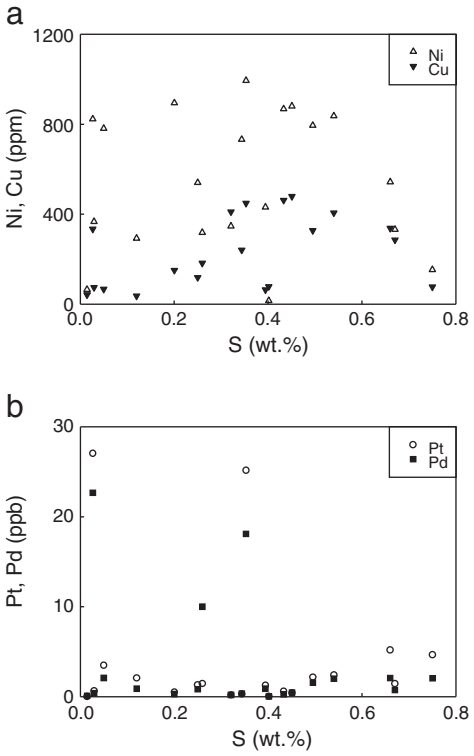

Fig. 7. Plots of S versus Ni, Cu (a) and Pt, Pd (b) for the Hongge intrusion.

crystallizing from magma or a magmatic sulfide liquid) or secondary (i.e., related to postmagmatic hydrothermal alteration). IPGE may crystallize as discrete minerals directly from silicate magma (Ballhaus and Sylvester, 2000; Ballhaus et al., 2006; Cawthorn, 1999; Keays, 1982; Keays and Campbell, 1981; Maier and Barnes, 1999; Melcher et al., 1997; Sattari et al., 2002; Tredoux et al., 1985) but PPGE will not crystallize as discrete minerals from the magma

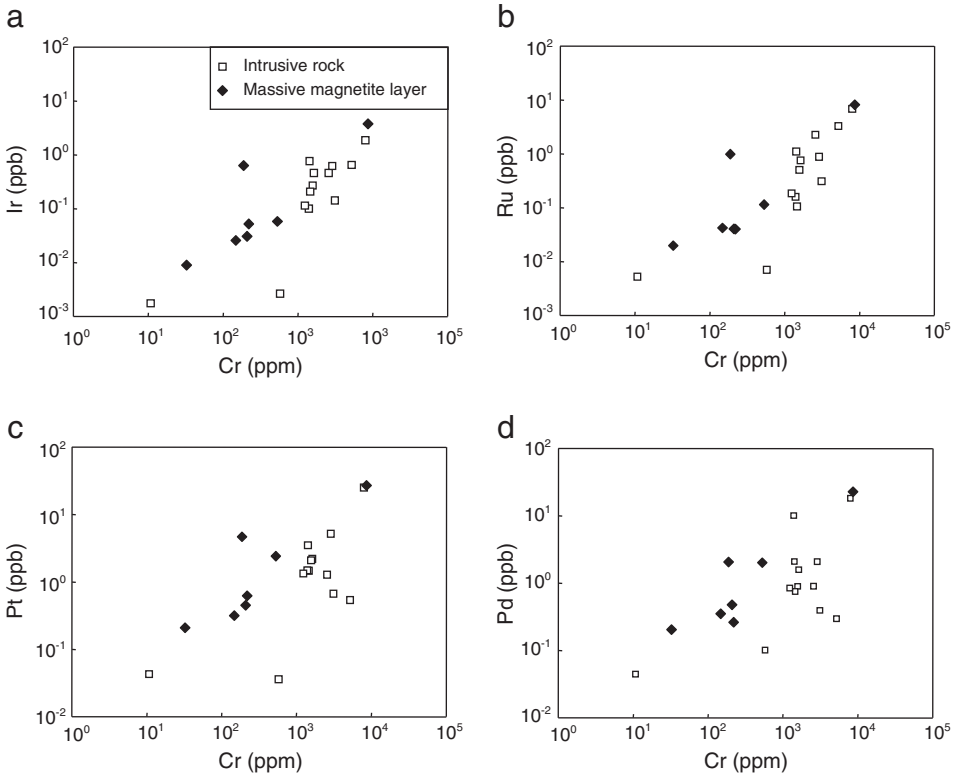

Fig. 6. Plots of Cr versus Ir (a), Ru (b), Pt (c), Pd (d) of the Hongge intrusion, showing positive correlations between Cr and Ir, Ru.

unless their concentrations in the magma are unusually high (i.e., much higher than a mantle-derived, PGE undepleted magma). Liang et al. (1998) reported the occurrence of sperrylites, vincentites and (Ru, Os)S_2 in the sulfide-bearing horizons of the Hongge intrusion, but the origin of these PGM are not clear. Given that most of the samples from the Hongge intrusion are PGE-poor, it is unlikely that the parental magma was saturated with Pt and Pd minerals. Thus, we believe that except the chromite-bearing samples, sulfide liquid was the main control of PGE distribution in the Hongge intrusion. It is also possible that the compositions of sulfide liquids in the different oxide-rich layers of the Hongge intrusion are variable. No correlations between PGE and S in the oxide-rich, sulfide-bearing layers in the Hongge intrusion can be explained by multiple sulfide liquids with different PGE compositions. This interpretation is supported by the fact that IPGE and PPGE are positively correlated in the samples (Fig. 8). Both IPGE and PPGE have large partition coefficients between sulfide liquid and silicate melts (see a compilation by Naldrett, 2011), and so they should produce positive correlation in the sulfide-bearing samples.

No correlations between PGE and S in the Hongge samples may be in part due to the involvement of multiple sulfide liquids with variable PGE compositions. In addition, it is possible that loss of S due to sulfide–oxide re-equilibration on cooling or post-magmatic hydrothermal alteration. Naldrett et al. (2012) suggested that non-stoichiometric magnetite may gain additional Fe from sulfide to fill the Fe^{2+} vacancies, resulting in loss of S in the assemblage. PGE redistribution during post-magmatic hydrothermal alteration (see examples given by Li et al., 2004, 2008) can also cause decoupling between PGE and S. Hydrothermal alteration is documented in the Hongge intrusion, so we cannot rule out this decoupling effect on PGE and S.

Two samples (MCZ15 and HG03) have unusually low Pt/Pd ratios as compared to the rest of the samples. Pt depletion relative to Pd is common in some magmatic sulfide ores that have experienced post-magmatic hydrothermal alteration. Examples of this include the Jinchuan Ni–Cu deposit in Gansu, China (Li and Ripley, 2011) and the Tianyu Ni–Cu sulfide deposit in Xinjiang, China (Tang et al., 2011). In magmatic sulfide ores, Pd is mainly hosted in pentlandite whereas Pt occurs predominantly as discrete PGM such as arsenide and telluride minerals. Their responses to postmagmatic hydrothermal leaching can be dramatically different, thereby resulting in local Pt and Pd decoupling. On the other hand, Pd is much more soluble than Pt in typical hydrothermal fluids and therefore more mobile, which can also cause decoupling between Pt and Pd (Barnes and Liu, 2012).

The experiments of Brenan et al. (2012) indicated that IPGE especially Ru strongly partition into spinel, with partition coefficients of 4–35 (D_{Ru}) between spinel and magma and positive with fO_2. In contrast, Pt and Pd are incompatible in spinel structure and their abundances increase in the fractionated magma during spinel crystallization. Harney et al. (1990) reported the enrichments of Os, Ir, and Ru in some magnetite-rich horizons in Upper Zone of the Bushveld Complex. However, this is not seen in the Hongge intrusion. As shown in Fig. 9a, no IPGE enrichments are present in the magnetite layers of the Hongge intrusion. The Pd/Ir ratios in the magnetite-rich samples of the Hongge intrusion are equal or greater than those of the associated magnetite-poor silicate rocks. This is because the magnetite layers in the Hongge intrusion contain variable amounts of disseminated sulfides which are more important than magnetite in controlling PGE distribution.

6.2. The nature of Hongge parental magma

It has been suggested that the parental magmas of the Fe–Ti–V oxide-bearing layered intrusions in the ELIP (e.g., Hongge, Panzhihua, Xinjie and Baima) are similar to the coeval high-Ti basalts and that they are all related to a common picritic magma by fractionation at depth (Pang et al., 2008a,b, 2009; Wang et al., 2008; Zhou et al., 2008). Chung and Jahn (1995) and Zhang et al. (2006) pointed out that the Emeishan picritic lavas have high Ti/Y ratios (~502–767) similar to that of the coeval high-Ti basalts analyzed by Xu et al. (2001) and Xiao et al. (2004a). As shown above, an important feature

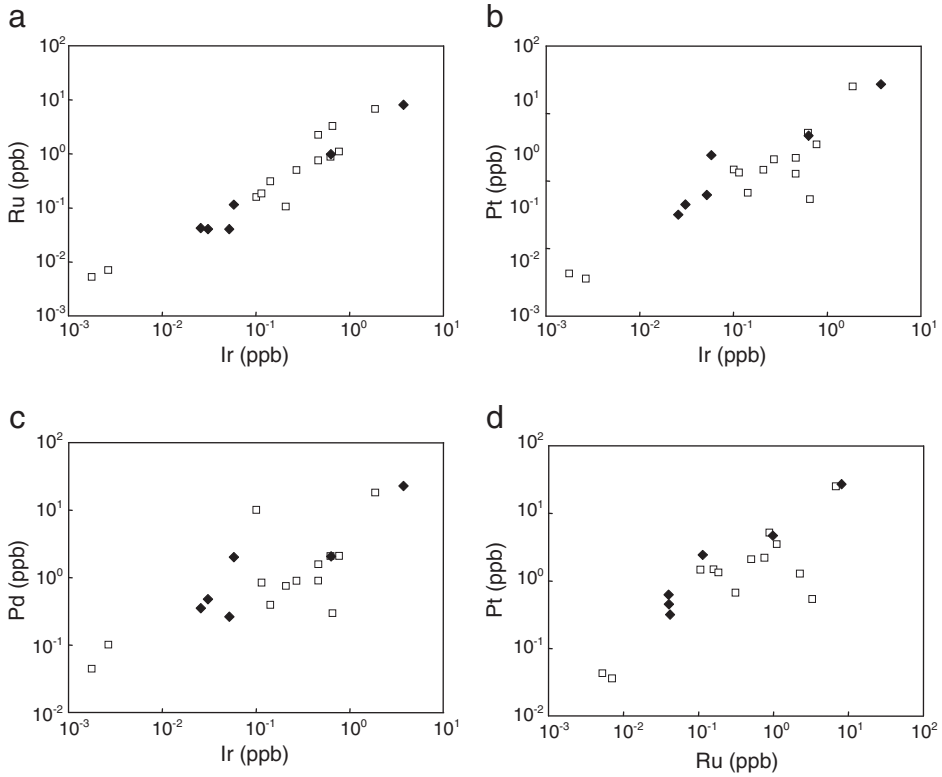

Fig. 8. Plots of Ir versus Ru (a), Pt (b), Pd (c) and Ru versus Pt (d) for the Hongge intrusion, showing positive correlations between individual PGEs.

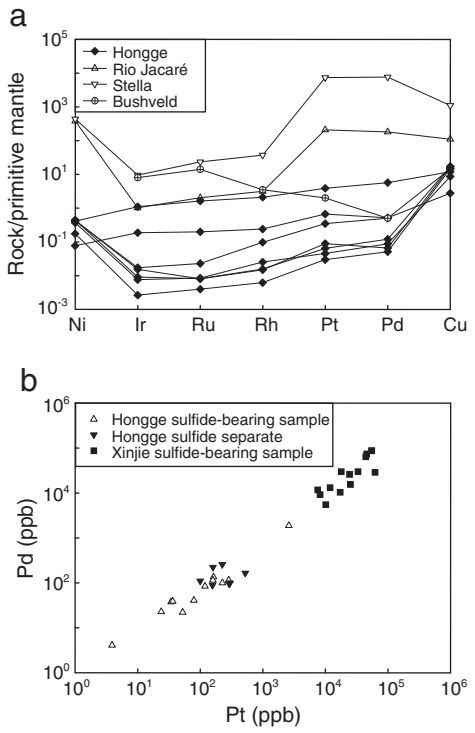

Fig. 9. (a) Comparison of primitive mantle-normalized PGE patterns for magnetite-rich rocks between the Hongge intrusion and other mafic–ultramafic intrusions in the world. The primitive mantle values are from Barnes and Maier (1999). The values for the Bushveld, Stella and Rio Jacaré intrusions are from Harney et al. (1990), Maier et al. (2003) and Sa et al. (2005), respectively. (b) Plots of Pt versus Pd tenors (in recalculated 100% sulfides) for the Hongge and Xinjie intrusions. The values for the Xinjie intrusion are from Zhong et al. (2011); the values of sulfide separates from the Hongge intrusion are from PXGT (1987).

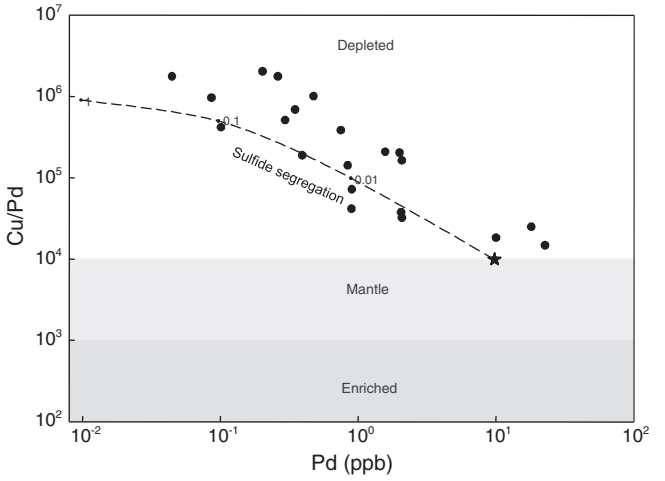

Fig. 10. Plot of Cu/Pd versus Pd for the Hongge intrusion and the coeval picrites from the Lijiang area, the Emeishan large igneous province.

of the Hongge layered intrusion is that the mantle-normalized PGE patterns are remarkably similar to those of the coeval high-Ti picrites in the region (see Fig. 5). This supports the notion that the parental magma of the Hongge intrusion may be related to the high-Ti picritic lavas by olivine fractional crystallization at depth. Compared to the coeval high-Ti basalts analyzed by Zhong et al. (2006) and Song et al. (2009), the primitive mantle normalized PGE patterns of the Hongge samples are less fractionated (see Fig. 5) and have lower Pd/Ir ratios, indicating that the parental magma of the Hongge intrusion is less fractionated than the coeval high-Ti basalts. This is supported by the fact that olivine is common in the Hongge intrusion but rare in the coeval high-Ti basalts. Using the composition of a coeval picrite sample containing olivine phenocrysts of ~Fo89 given by Chung and Jahn (1995) and Xu and Chung (2001) as a starting composition, our calculations using the MELTS program of Ghiorso and Sack (1995) indicate that about 22% of fractional crystallization at crustal levels is required to produce a fractionated magma that can crystallize olivine with composition similar to that seen in the Hongge intrusion (i.e., ~Fo82, Bai et al., in press).

The compositions of chalcophile elements in a mantle-derived, primitive magma are mainly controlled by the degree of partial melting in the mantle (Arndt et al., 2005; Barnes and Lightfoot, 2005; Barnes and Maier, 1999; Naldrett, 2010a,b). Pd partitions more strongly into a sulfide liquid than Cu during sulfide segregation from magma (see partition coefficients compiled by Naldrett, 2011). If sulfide liquid is present during mantle partial melting, the magma will be depleted in Pd relative to Cu. As shown in Fig. 10, the Cu/Pd ratios (~9900) of the Emeishan picrites are similar to that of the primitive mantle (Cu/Pd = 10^3–10^4: Barnes et al., 1993), indicating that sulfide was not present in the source mantle which had experienced relatively high degree of partial melting.

It has been suggested that the mantle contains ~250 ppm S (McDonough and Sun, 1995) or 0.054 wt.% sulfide (Lorand, 1993). To dissolve all sulfides in the mantle-derived magma, ~18% (Naldrett, 2010b) or ~25% (Keays, 1995) of partial melting in the mantle is required. However, different opinions of magma generation exist for the ELIP. Xu et al. (2001) and Zhang et al. (2006) suggested that the high-Ti basalts and picritic lavas were generated by 1.5% partial melting in the mantle plume periphery and ~2–7% in plume head, respectively. Xiao et al. (2004a) suggested that the high-Ti basalts were also produced by low degrees of partial melting in the plume head. Wang et al. (2007) suggested the degree of partial melting was probably less than ~8% for the parental magmas of the high-Ti basalts. In contrast, much higher degrees of mantle partial melting for the volcanic rocks, especially the least-fractionated samples, have also been proposed (10–20%: Qi and Zhou, 2008; Song et al., 2009). All these estimations are mainly based on rare earth element data. Given the fact that some picrite samples in the ELIP have Cu/Pd ratios similar to that of the primitive mantle (Table 1), we believe that a higher degree of mantle partial melting (>15%) is more plausible for these samples.

Bai et al. (in press) suggested that the primitive/parental magma of the Hongge intrusion is similar to the average composition of the Pechenga ferropicrites/ferrobasalts in terms of major-trace element compositions and Sm–Nd isotopes. Zhong et al. (2011) suggested that the parental magma of these magnetite-enriched intrusions formed by interaction of a mantle plume-derived magma with previously subducted oceanic crust (probably <10%) during ascent. In this model, high FeO and TiO_2 contents in the magma are thought to have resulted from selective assimilation of oxides from the oceanic crust that was subducted shortly before the arrival of the Emeishan mantle plume (Zhong et al., 2011).

6.3. PGE depletion in the Hongge intrusion

Magnetite-bearing layers formed from a highly fractionated magma in the upper parts of layered intrusions worldwide are often depleted in PGE due to extremely low PGE contents in the magma. However, PGE enrichments in magnetite horizons have been reported for several mafic–ultramafic intrusions. For examples, the magnetite layers of the Rio Jacaré intrusion in northern Brazil contain up to 208 ppb Pt and 181 ppb Pd in the Rio (Sa et al., 2005), the oxide zone in the Stella intrusion in South Africa contains 7.3 ppm Pt and 7.6 ppm Pd (Maier et al., 2003) (Fig. 9a). The PGE enrichments within the magnetite-rich horizons have also been found in the Platinova reef of the Skaergaard intrusion, Greenland (Andersen, 2006;

Andersen et al., 1998; Brooks et al., 1999; Nielsen and Brooks, 1995) and the Rincón del Tigre Complex, Eastern Bolivia (Prendergast, 2000). In the ELIP, magnetite layers with high PGE contents (up to 1.2 ppm Pt and 1.8 ppm Pd) have been found in the Xinjie Fe–Ti oxide-bearing mafic–ultramafic layered intrusion (Zhong et al., 2011). The PGE-enriched magnetite layers in the Xinjie intrusion are characterized by the presence of disseminated sulfides. It is rather surprising that none of the magnetite layers in the Hongge intrusion we have studied to date have high PGE concentrations despite the fact that they also contain disseminated sulfides.

The magnetite reef in the Kiglapait Complex of the Nain Plutonic Suite, Labrador, which formed at about 88% crystallization in a closed system (Morse, 1979, 1981), has no PGE enrichment (Lightfoot et al., 2012). Lightfoot et al. (2012) suggested a PGE-depleted parental magma for the Kiglapait mafic intrusion and proposed that PGE depletion in the magma was due to sulfide retention in the source mantle. This model cannot explain the PGE depletion in the Hongge intrusion because some of the coeval volcanic rocks (Song et al., 2009; Zhang et al., 2005; Zhong et al., 2006) with compositions similar to the parental magmas of the Hongge intrusion and other coeval mafic–ultramafic intrusions in the region (Pang et al., 2008a,b, 2009; Wang et al., 2008; Zhou et al., 2008) are not depleted in PGE (Fig. 5). As mentioned above, some sulfide-bearing magnetite layers in the coeval Xinjie intrusion contain elevated PGE. We believe that the contrasting PGE abundances in the magnetite layers of these two intrusions mainly reflect different sulfide liquid compositions which in turn reflect different PGE abundances in their respective parental magmas. The parental magma of the Xinjie intrusion is not depleted in PGE due to absence of previous sulfide saturation and segregation at depth. The parental magma of the Hongge intrusion was also more evolved than that of the Xinjie intrusion based on olivine composition (~Fo82 versus ~Fo88: Zhang et al., 2009). We suggest that PGE depletion in the Hongge intrusion is due to a previous event of sulfide saturation and segregation prior to magma emplacement at Hongge. As discussed above, immiscible sulfide liquid segregation from magma will dramatically deplete PGE in the magma owing to their extremely high partition coefficients between sulfide liquid and magma (see the partition coefficients compiled by Naldrett, 2011). As a result, any second-stage sulfide liquid segregated from the PGE depleted magma will be extremely depleted in PGE. This can explain the low PGE tenors in the bulk sulfides (i.e., in recalculated 100% sulfides) of the Hongge intrusion. Compared to the Xinjie intrusion, the PGE tenors of bulk sulfides for the sulfide-bearing samples (>1% total sulfides) from the Hongge intrusion are close to 3 order of magnitudes lower (<0.1–3 ppm versus 10–100 ppm) (see Fig. 9b). Extremely low PGE tenors in the bulk sulfides of the Hongge intrusion have been known for some times (e.g., Zhong et al., 2002). A previous study reported 0.533 ppm total PGE for sulfide separates from the Hongge intrusion (PXGT, 1987).

6.4. Sulfide saturation history

Timing of sulfide saturation during magma evolution is critical in the formation of PGE–rich magmatic sulfide ores (Arndt et al., 2005; Barnes and Lightfoot, 2005). As pointed out by Barnes and Maier (1999), Cu/Pd ratio is a good tool to evaluate sulfide saturation history in magma. Owing to a much higher partition coefficient for Pd than Cu between sulfide liquid and magma, a second-stage sulfide liquid will have much higher Cu/Pd ratio than that of the primitive mantle. The Cu/Pd ratios of the Hongge samples range from ~1.47×10^4 to 2.02×10^6 (Fig. 10), significantly higher than the mantle ratio (10^3–10^4, Barnes et al., 1993) as well as the coeval Emeishan picrites (~9900). This supports our interpretation that the sulfides in the magnetite layers of the Hongge intrusion formed by second-stage sulfide liquid segregation from a PGE-depleted magma that experienced previous sulfide segregation at depth. Our calculations indicate that the amount of sulfide liquid segregated in the first stage is ~0.1 wt.% (Fig. 10). Such weakly S-saturated magmas experienced much less than 1% sulfide removal were also reported at Noril'sk (Lightfoot and Keays, 2005).

Sulfide saturation of magma may result from (1) fractional crystallization, (2) magma mixing, and (3) crustal contamination. Sulfur is an incompatible element in olivine, clinopyroxene and chromite, and will increase in the residual magma during fractional crystallization. The sulfur content at sulfide saturation (SCSS) in magma is mainly controlled by temperature, pressure and composition, especially FeO content of the magma (e.g., Li and Ripley, 2005; Mavrogenes and O'Neill, 1999). Mathez (1976) suggested that the S solubility in MORB magma increases during fractional crystallization of plagioclase and olivine because the FeO content in the magma increases. However, our calculations using the equation of Li and Ripley (2009) in which the effects of both FeO content and temperature are included indicate that the SCSS decreases during fractional crystallization of the parental magma for the Hongge intrusion (Fig. 11). In our calculation we used the composition of a representative picrite sample from the ELIP given by Chung and Jahn (1995) as a starting composition. The results of our calculations indicate that at least 42% of fractional crystallization is required to induce sulfide saturation if no external S is involved. This value is much higher than the value suggested by the difference in Fo contents between olivine in the picrite and the Hongge intrusion (~22%), which implies that fractional crystallization did not play a major role in sulfide saturation in the Hongge magmatic system. This interpretation is supported by the fact that some coeval fractionated high-Ti basalts in the region are not depleted in PGE (Fig. 5, Song et al., 2009).

Mixing between a resident magma in the chamber with a new replenishment of more primitive magma may cause sulfide saturation (Campbell et al., 1983; Li et al., 2001; Naldrett and von Gruenewaldt, 1989). Based on the significant reversal of elemental ratios at the base of some magnetite layers in the Hongge intrusion, Zhong et al. (2002, 2003) suggested magma mixing may have taken place during the formation of the magnetite layers in the intrusion. However, as pointed out by Li and Ripley (2005), sulfide saturation may not occur during magma mixing if one of the end-members is significantly S-undersaturated. Although this process may explain the origin of the PGE-depleted sulfides in the Hongge intrusion, but

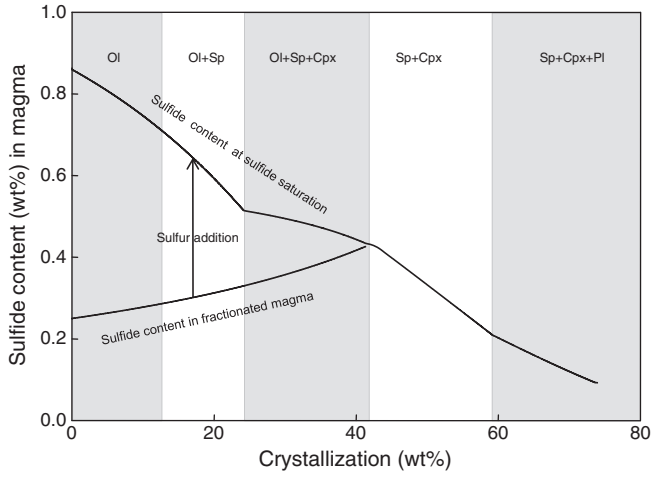

Fig. 11. Sulfur content at sulfide saturation (SCSS) during magma evolution. The starting composition is based on an Emeishan picrite sample EM55 analyzed by Chung and Jahn (1995). Fractional crystallization was simulated using the MELTS program of Ghiorso and Sack (1995) at 1 kbar and under the assumed oxidation state of FMQ buffer. The SCSS curve is generated using the equation of Li and Ripley (2009). The initial sulfide content in the magma is assumed to be 0.25 wt.%. Ol, olivine; Sp, spinel; Cpx, clinopyroxene; Pl, plagioclase.

the cause of the previous sulfide saturation event (i.e., the first-stage) at depth needs another explanation.

Contamination by country rocks has been widely regarded as an important trigger for sulfide saturation during magma evolution in the ELIP (Song et al., 2003; Tao et al., 2008; Wang et al., 2006; Zhong et al., 2004). The importance of this process in form of selective S assimilation during magma evolution in the Hongge magmatic system is highlighted in Fig. 11. The mafic metavolcanic rocks of the Paleo-Mesoproterozoic Huili Group hosting VMS deposits (e.g., Lala copper deposit; He et al., 2010) in this area may have provided the external S to the magma to induce the first-stage of sulfide saturation in the magma plumbing system at depth. The isotopic data of the Hongge intrusion ($\varepsilon_{Nd}(t) = -1.03$ to $+1.02$; Zhong et al., 2003) indicate that the parental magma of the Hongge intrusion experienced significant crust contamination. Thus, we believe that the first-stage sulfide segregation in the Hongge magmatic system at depth was mainly induced by crustal contamination. Due to the negative pressure effect on the SCSS (e.g., Mavrogenes and O'Neill, 1999), a sulfide-saturated magma will become sulfide undersaturated again during ascent. Further fractional crystallization involving abundant magnetite at Hongge could have reduced FeO content in the magma and thus induced sulfide saturation. The close association between sulfides and magnetite in the Hongge intrusion is consistent with this interpretation. Similar interpretation has been proposed previously for the sulfide–magnetite mineralization in some mafic–ultramafic intrusions elsewhere in the world (Andersen, 2006; Andersen et al., 1998; Brooks et al., 1999; Jenner et al., 2010; Maier et al., 2003; Nielsen and Brooks, 1995; Prendergast, 2000).

7. Conclusions

The main conclusions from this study are summarized below.

(1) The magnetite-rich layers of the Hongge intrusion have primitive mantle-normalized PGE patterns similar to that of the Emeishan picritic lavas but are characterized by much lower PGE abundances than the coeval volcanic rocks.
(2) Copper and PGE distribution in the Hongge intrusion are inferred to have originally controlled by immiscible sulfide liquids except the chromite-bearing samples in which IPGE are also controlled by the abundance of chromite.
(3) No IPGE enrichments relative to PPGE are observed in the magnetite ores of the Hongge intrusion. This, together with similar PGE contents between the magnetite ores and associated rocks, indicates that Fe–Ti oxides are not the major collectors of IPGE in the Hongge intrusion.
(4) The PGE tenors in bulk sulfide (i.e., in recalculated 100% sulfides) in the sulfide-bearing oxide ores are close to 3 orders of magnitude lower than those in the Xinjie intrusion. This, together with much higher Cu/Pd ratios in the Hongge samples, indicates that the parental magma of the Hongge intrusion was depleted in PGE, possibly due to previous sulfide segregation at depth. The sulfides in the Hongge intrusion formed by second-stage sulfide liquid segregation from the PGE-depleted magma.
(5) The two sulfide saturation events in the Hongge magma are thought to have resulted from crustal contamination at depth, and from further fractional crystallization involving abundant magnetite after magma emplacement at Hongge, respectively.

Acknowledgments

We appreciate the assistance of Dr. Liang Qi in PGE analysis. Drs. Peter Lightfoot and Steve Barnes, and Editor Prof. Nigel Cook are thanked for their constructive reviews. This study was jointly supported by the National Basic Research Program of China (2007CB411401), the Knowledge-Innovation Program of the Chinese Academy of Sciences (KZCX2-YW-136), the "CAS Hundred Talents" Foundation of the Chinese Academy of Sciences to HZ, the National Natural Science Foundation of China (40873028), and the State Key Laboratory of Ore Deposit Geochemistry of China (2009–05).

Appendix

Supplementary data 1. Analytical results, blank and detection limits (DL) of PGE (in ppb) for reference material WGB-1.

Elements	Blank		WGB-1			
	Measured	DL	Measured	Qi et al. (2008)	Meisel and Moser (2004)	Certified
Ir	0.0017	0.001	0.16	0.16 ± 0.02	0.21	0.33
Ru	0.0124	0.001	0.12	0.13 ± 0.01	0.14	0.3
Rh	0.0019	0.001	0.22	0.20 ± 0.02	0.23	0.32
Pt	0.0015	0.009	5.39	6.34 ± 0.61	6.39	6.1
Pd	0.0396	0.015	13.84	13.0 ± 1.1	13.9	13.9

Certified = Govindaraju (1994).

References

Andersen, J.C.Ø., 2006. Postmagmatic sulphur loss in the Skaergaard Intrusion: implications for the formation of the Platinova Reef. Lithos 92, 198–221.
Andersen, J.C.Ø., Rasmussen, H., Nielsen, T.F.D., Ronsbo, J.G., 1998. The Triple Group and the Platinova gold and palladium reefs in the Skaergaard Intrusion; stratigraphic and petrographic relations. Econ. Geol. 93, 488–509.
Arndt, N.T., Lesher, C.M., Czamanske, G., 2005. Mantle-derived magmas and magmatic Ni–Cu–(PGE) deposits. Economic Geology 100th Anniversary Volume, pp. 5–23.
Bai Z.J., Zhong H., Naldrett A.J., Zhu W.G., Xu G.W., in press. Whole rock and mineral composition constraints on the genesis of the giant Hongge Fe–Ti–V oxide deposit in the Emeishan Large Igneous Province, SW China. Economic Geology.
Ballhaus, C., Sylvester, P., 2000. Noble metal enrichment processes in the Merensky reef, Bushveld complex. J. Petrol. 41, 545–561.
Ballhaus, C., Bockrath, C., Wohlgemuth-Ueberwasser, C., Laurenz, V., Berndt, J., 2006. Fractionation of the noble metals by physical processes. Contrib. Mineral. Petrol. 152, 667–684.
Barnes, S.-J., Lightfoot, P.C., 2005. Formation of magmatic nickel sulfide ore deposits and processes affecting their copper and platinum group element contents. Economic Geology 100th Anniversary Volume, pp. 179–214.
Barnes, S.J., Liu, W.H., 2012. Pt and Pd mobility in hydrothermal fluids: evidence from komatiites and from thermodynamic modelling. Ore Geol. Rev. 44, 49–58.
Barnes, S.-J., Maier, W.D., 1999. The fractionation of Ni, Cu and the noble metals in silicate and sulphide liquids. In: Keays, R.R., Lesher, C.M., Lightfoot, P.C., Farrow, C.E.G. (Eds.), Dynamic Processes in Magmatic Ore Deposits and Their Application to Mineral Exploration: Geological Association of Canada, Short Course Notes, Volume 13, pp. 69–106.
Barnes, S.-J., Picard, C.P., 1993. The behaviour of platinum-group elements during partial melting, crystal fractionation, and sulphide segregation: an example from the Cape Smith Fold Belt, northern Quebec. Geochim. Cosmochim. Acta 57, 79–87.
Barnes, S.-J., Naldrett, A.J., Gorton, M.P., 1985. The origin of the fractionation of platinum-group elements in terrestrial magmas. Chem. Geol. 53, 303–323.
Barnes, S.-J., Couture, J.F., Sawyer, E.W., Bouchaib, C., 1993. Nickel–copper occurrences in the Belleterre–Angliers Belt of the Pontiac Subprovince and the use of Cu–Pd ratios in interpreting platinum-group element distributions. Econ. Geol. 88, 1402–1418.
Bezmen, N.I., Asif, M., Brugmann, G.E., Romanenko, I.M., Naldrett, A.J., 1994. Distribution of Pd Rh Ru Ir Os and Au between sulfide and silicate melts. Geochim. Cosmochim. Acta 58, 1251–1260.
Brenan, J.M., McDonough, W.F., Dalpé, C., 2003. Experimental constraints on the partitioning of rhenium and some platinum-group elements between olivine and silicate melt. Earth Planet. Sci. Lett. 212, 135–150.
Brenan, J.M., McDonough, W.F., Ash, R., 2005. An experimental study of the solubility and partitioning of iridium, osmium and gold between olivine and silicate melt. Earth Planet. Sci. Lett. 237, 855–872.
Brenan, J.M., Finnigan, C.F., McDonough, W.F., Homolova, V., 2012. Experimental constraints on the partitioning of Ru, Rh, Ir, Pt and Pd between chromite and silicate melt: the importance of ferric iron. Chem. Geol.. doi:10.1016/j.chemgeo.2011.05.015
Brooks, C.K., Keays, R.R., Lambert, D.D., Frick, L.R., Nielsen, T.F.D., 1999. Re–Os isotope geochemistry of Tertiary picritic and basaltic magmatism of East Greenland: constraints on plume–lithosphere interactions and the genesis of the Platinova reef, Skaergaard intrusion. Lithos 47, 107–126.
Campbell, I.H., Naldrett, A.J., Barnes, S.J., 1983. A model for the origin of the platinum-rich sulfide horizons in the Bushveld and Stillwater Complexes. J. Petrol. 24, 133–165.

Cawthorn, R.G., 1999. Platinum-group element mineralization in the Bushveld Complex — a critical reassessment of geochemical models. S. Afr. J. Geol. 102, 268–281.
Chung, S.L., Jahn, B.M., 1995. Plume–lithosphere interaction in generation of the Emeishan flood basalts at the Permian–Triassic boundary. Geology 23, 889–892.
Crocket, J.H., Fleet, M.E., Stone, W.E., 1997. Implications of composition for experimental partitioning of platinum-group elements and gold between sulfide liquid and basalt melt: the significance of nickel content. Geochim. Cosmochim. Acta 61, 4139–4149.
Fleet, M.E., Crocket, J.H., Stone, W.E., 1996. Partitioning of platinum group elements (Os, Ir, Ru, Pt, Pd) and gold between sulfide liquid and basalt melt. Geochim. Cosmochim. Acta 60, 2397–2412.
Fonseca, R.O.C., Campbell, I.H., O'Neill, H.S.C., Allen, C.M., 2009. Solubility of Pt in sulphide mattes: implications for the genesis of PGE-rich horizons in layered intrusions. Geochim. Cosmochim. Acta 73, 5764–5777.
Francis, R.D., 1990. Sulfide globules in mid-ocean ridge basalts (MORB), and effect of oxygen abundance in Fe–S–O liquids on the ability of those liquids to partition metals from MORB and komatiite magmas. Chem. Geol. 85, 199–213.
Gaetani, G.A., Grove, T.L., 1997. Partitioning of moderately siderophile elements among olivine sulfide melt and silicate melt: constraints on core formation in the Earth and Mars. Geochim. Cosmochim. Acta 61, 1829–1846.
Ghiorso, M.S., Sack, R.O., 1995. Chemical mass transfer in magmatic processes IV. A revised and internally consistent thermodynamic model for the interpolation and extrapolation of liquid–solid equilibria in magmatic systems at elevated temperatures and pressures. Contrib. Mineral. Petrol. 119, 197–212.
Govindaraju, K., 1994. 1994 compilation of working values and sample description for 383 geostandards: Geostandards and Geoanalytical Research, 18. 158 pp.
Guo, F., Fan, W.M., Wang, Y.J., Li, C.W., 2004. When did the Emeishan mantle plume activity start? Geochronological and geochemical evidence from ultramafic–mafic dikes in Southwestern China. Int. Geol. Rev. 46, 226–234.
Harney, D.M.W., Merkle, R.K.W., Von Gruenewaldt, G., 1990. Platinum-group element behavior in the lower part of the upper zone, Eastern Bushveld Complex; implications for the formation of the main magnetite layer. Econ. Geol. 85, 1777–1789.
He, D.F., Zhong, H., Zhu, W.G., Xiao, F., 2010. Geochemical characteristics of the ore-bearing strata metasedimentary host rocks in the Lala copper deposit, Sichuan Province. Earth Sci. Front. 17, 218–226 (in Chinese with English abstract).
Jenner, F.E., O'Neill, H.S.C., Arculus, R.J., Mavrogenes, J.A., 2010. The magnetite crisis in the evolution of arc-related magmas and the initial concentration of Au, Ag and Cu. J. Petrol. 51, 2445–2464.
Keays, R.R., 1982. Palladium and iridium in komatiites and associated rocks: application to petrogenetic problems. In: Arndt, N.T., Nisbet, E.G. (Eds.), Komatiites. Springer, Berlin, pp. 435–457.
Keays, R.R., 1995. The role of komatiitic and picritic magmatism and S-saturation in the formation of ore deposits. Lithos 34, 1–18.
Keays, R.R., Campbell, I.H., 1981. Precious metals in the Jimberlana Intrusion, western Australia; implications for the genesis of platiniferous ores in layered intrusions. Econ. Geol. 76, 1118–1141.
Li, C., Ripley, E.M., 2005. Empirical equations to predict the sulfur content of mafic magmas at sulfide saturation and applications to magmatic sulfide deposits. Miner. Deposita 40, 218–230.
Li, C., Ripley, E.M., 2009. Sulfur contents at sulfide–liquid or anhydrite saturation in silicate melts: empirical equations and example applications. Econ. Geol. 104, 405–412.
Li, C., Ripley, E.M., 2011. The Giant Jinchuan Ni–Cu–(PGE) deposit: tectonic setting, magma evolution, ore genesis and exploration implications. In: Li, C., Ripley, E.M. (Eds.), Magmatic Ni–Cu and PGE deposits: geology, geochemistry and genesis: Reviews in Economic Geology, 17, pp. 163–180.
Li, C., Maier, W.D., de Waal, S.A., 2001. The role of magma mixing in the origin of PGE mineralization in the Bushveld Complex: thermodynamic calculations and new interpretations. Econ. Geol. 96, 653–662.
Li, Z.X., Li, X.H., Kinny, P.D., Wang, J., Zhang, S., Zhou, H., 2003. Geochronology of Neoproterozoic syn-rift magmatism in the Yangtze Craton, South China and correlations with other continents: evidence for a mantle superplume that broke up Rodinia. Precambrian Res. 122, 85–109.
Li, C., Ripley, E.M., Merino, E., Maier, W.D., 2004. Replacement of base metal sulfides by actinolite, epidote, calcite, and magnetite in the UG2 and Merensky reef of the Bushveld complex, South Africa. Econ. Geol. 99, 173–184.
Li, X.H., Li, Z.X., Sinclair, J.A., Li, W.X., Carter, G., 2006. Revisiting the "Yanbian Terrane": implications for Neoproterozoic tectonic evolution of the western Yangtze Block, South China. Precambrian Res. 151, 14–30.
Li, C., Ripley, E.M., Oberthür, T., Miller, J.D., Joslin, G.D., 2008. Textural and stable isotope studies of hydrothermal alteration in the Main Sulfide Zone of the Great Dyke, Zimbabwe, and the Precious Metals Zone of the Sonju Lake Intrusion, Minnesota, USA. Miner. Deposita 43, 97–110.
Liang, Y.B., Liu, T.Y., Song, G.R., Jin, Z.M., 1998. Platinum Group Element Deposits in China. Metallurgical Industry Press, Beijing. (in Chinese).
Lightfoot, P.C., Keays, R.R., 2005. Siderophile and chalcophile metal variations in flood basalts from the Siberian trap, Noril'sk region: implications for the origin of the Ni–Cu–PGE sulfide ores. Econ. Geol. 100, 439–462.
Lightfoot, P.C., Keays, R.R., Evans-Lamswood, D., Wheeler, R., 2012. S saturation history of Nain Plutonic Suite mafic intrusions: origin of the Voisey's Bay Ni–Cu–Co sulfide deposit, Labrador, Canada. Miner. Deposita 47, 23–50.
Locmelis, M., Pearson, N.J., Barnes, S.J., Fiorentini, M.L., 2011. Ruthenium in komatiitic chromite. Geochim. Cosmochim. Acta 75, 3645–3661.
Lorand, J.P., 1993. Comment on "Content and isotopic composition of sulphur in ultramafic xenoliths from central Asia" by D.A. Ionov, J. Hoefs, K.H. Wedepohl, U. Wiechert. Discussion. Earth Planet. Sci. Lett. 119, 627–634.
Maier, W.D., Barnes, S.-J., 1999. Platinum-group elements in silicate rocks of the lower, critical and main zones at union section, western Bushveld complex. J. Petrol. 40, 1647–1671.
Maier, W.D., Barnes, S.-J., Gartz, V., Andrews, G., 2003. Pt–Pd reefs in magnetitites of the Stella layered intrusion, South Africa: a world of new exploration opportunities for platinum group elements. Geology 31, 885–888.
Mathez, E.A., 1976. Sulfur solubility and magmatic sulfides in submarine basalt glass. J. Geophys. Res. 81, 4269–4276.
Mavrogenes, J.A., O'Neill, H.St.C., 1999. The relative effects of pressure, temperature and oxygen fugacity on the solubility of sulfide in mafic magmas. Geochim. Cosmochim. Acta 63, 1173–1180.
McDonough, W.F., Sun, S.S., 1995. The composition of the Earth. Chem. Geol. 120, 223–253.
Meisel, T., Moser, T., 2004. Reference materials for geochemical PGE analysis: new analytical data for Ru, Rh, Pd, Os, Ir, Pt and Re by isotope dilution ICP-MS in 11 geological reference materials. Chem. Geol. 208, 319–338.
Melcher, F., Grum, W., Simon, G., Thalhammer, T.V., Stumpfl, E.F., 1997. Petrogenesis of the ophiolitic giant chromite deposits of Kempirsai, Kazakhstan: a study of solid and fluid inclusions in chromite. J. Petrol. 38, 1419–1458.
Morse, S.A., 1979. Kiglapait geochemistry I: systematics, sampling, and density. J. Petrol. 20, 555–590.
Morse, S.A., 1981. Kiglapait geochemistry IV: the major elements. Geochim. Cosmochim. Acta 45, 461–479.
Naldrett, A.J., 2010a. From the mantle to the bank: the life of a Ni–Cu–(PGE) sulfide deposit. S. Afr. J. Geol. 113, 1–32.
Naldrett, A.J., 2010b. Secular variation of magmatic sulfide deposits and their source magmas. Econ. Geol. 105, 669–688.
Naldrett, A.J., 2011. Fundamentals of magmatic sulfide deposits. In: Li, C., Ripley, E.M. (Eds.), Magmatic Ni–Cu and PGE Deposits: Geology, Geochemistry and Genesis: Reviews in Economic Geology, 17, pp. 1–50.
Naldrett, A.J., von Gruenewaldt, G., 1989. Association of platinum-group elements with chromitite in layered intrusions and ophiolite complexes. Econ. Geol. 84, 180–187.
Naldrett, A.J., Wilson, A., Kinnaird, J., Yudovskaya, M., Chunnett, G., 2012. The origin of chromitites and related PGE mineralization in the Bushveld Complex: new mineralogical and petrological constraints. Miner. Deposita. doi:10.1007/s00126-011-0366-3.
Nielsen, T.F.D., Brooks, C.K., 1995. Precious metals in magmas of East Greenland; factors important to the mineralization in the Skaergaard Intrusion. Econ. Geol. 90, 1911–1917.
Pagé, P., Barnes, S.-J., Bédard, J.H., Zientek, M.L., 2012. In situ determination of Os, Ir, and Ru in chromites formed from komatiite, tholeiite and boninite magmas: implications for chromite control of Os, Ir and Ru during partial melting and crystal fractionation. Chem. Geol.. doi:10.1016/j.chemgeo.2011.06.006
Pang, K.N., Li, C., Zhou, M.F., Ripley, E.M., 2008a. Abundant Fe–Ti oxide inclusions in olivine from the Panzhihua and Hongge layered intrusions, SW China: evidence for early saturation of Fe–Ti oxides in ferrobasaltic magma. Contrib. Mineral. Petrol. 156, 307–321.
Pang, K.N., Zhou, M.F., Lindsley, D., Zhao, D.G., Malpas, J., 2008b. Origin of Fe–Ti oxide ores in mafic intrusions: evidence from the Panzhihua intrusion, SW China. J. Petrol. 49, 295–313.
Pang, K.N., Li, C., Zhou, M.F., Ripley, E.M., 2009. Mineral compositional constraints on petrogenesis and oxide ore genesis of the late Permian Panzhihua layered gabbroic intrusion, SW China. Lithos 110, 199–214.
Peach, C.L., Mathez, E.A., 1996. Constraints on the formation of platinum-group element deposits in igneous rocks. Econ. Geol. 91, 439–450.
Peach, C.L., Mathez, E.A., Keays, R.R., 1990. Sulfide melt–silicate melt distribution coefficience for noble metals and other chalcophile elements as deduced from MORB: implications for partial melting. Geochim. Cosmochim. Acta 54, 3379–3389.
Peach, C.L., Mathez, E.A., Keays, R.R., Reeves, S.J., 1994. Experimentally determined sulfide melt–silicate melt partition coefficients for Ir and Pd. Chem. Geol. 117, 361–377.
Prendergast, M.D., 2000. Layering and precious metals mineralization in the Rincón del Tigre Complex, Eastern Bolivia. Econ. Geol. 95, 113–130.
Puchtel, I.S., Humayun, M., 2001. Platinum group element fractionation in a komatiitic basalt lava lake. Geochim. Cosmochim. Acta 65, 2979–2993.
PXGT, 1987. Metallogenetic Conditions and Geologic Characters of the Hongge Vanadic Titanomagnetite Deposit, Sichuan. Geological Publishing House, Beijing. 220 pp. (in Chinese).
Qi, L., Zhou, M.F., 2008. Platinum-group elemental and Sr–Nd–Os isotopic geochemistry of Permian Emeishan flood basalts in Guizhou Province, SW China. Chem. Geol. 248, 83–103.
Qi, L., Zhou, M.F., Wang, C.Y., 2004. Determination of low concentrations of platinum group elements in geological samples by ID-ICP-MS. J. Anal. At. Spectrom. 19, 1335–1339.
Qi, L., Zhou, M.F., Wang, C.Y., Sun, M., 2007. Evaluation of the determination of Re and PGEs abundance of geological samples by ICP-MS coupled with a modified Carius tube digestion at different temperatures. Geochem. J. 41, 407–414.
Qi, L., Wang, C.Y., Zhou, M.F., 2008. Controls on the PGE distribution of Permian Emeishan alkaline and peralkaline volcanic rocks in Longzhoushan, Sichuan Province, SW China. Lithos 106, 222–236.
Rajamani, V., Naldrett, A.J., 1978. Partitioning of Fe Co Ni and Cu between sulfide liquid and basaltic melts and the composition of Ni–Cu sulfide deposits. Econ. Geol. 73, 82–93.
Righter, K., Campbell, A.J., Humayun, M., Hervig, R.L., 2004. Partitioning of Ru, Rh, Pd, Re, Ir, and Au between Cr-bearing spinel, olivine, pyroxene and silicate melts. Geochim. Cosmochim. Acta 68, 867–880.

Sa, J.H.S., Barnes, S.-J., Prichard, H.M., Fisher, P.C., 2005. The distribution of base metals and platinum-group elements in magnetitite and its host rocks in the Rio Jacare intrusion, Northeastern Brazil. Econ. Geol. 100, 333–348.
Sattari, P., Brenan, J.M., Horn, I., McDonough, W.F., 2002. Experimental constraints on the sulfide- and chromite–silicate melt partitioning behavior of rhenium and platinum-group elements. Econ. Geol. 97, 385–398.
Song, X.Y., Zhou, M.F., Cao, Z.M., Sun, M., Wang, Y.L., 2003. Ni–Cu–(PGE) magmatic sulfide deposits in the Yangliuping area, Permian Emeishan Igneous Province, SW China. Miner. Deposita 38, 831–843.
Song, X.Y., Keays, R.R., Xiao, L., Qi, H.W., Ihlenfeld, C., 2009. Platinum-group element geochemistry of the continental flood basalts in the central Emeisihan Large Igneous Province, SW China. Chem. Geol. 262, 246–261.
Stone, W.E., Crocket, J.H., Fleet, M.E., 1990. Partitioning of palladium iridium platinum and gold between sulfide liquid and basalt melt at 1200°C. Geochim. Cosmochim. Acta 54, 2341–2344.
Tang, D.M., Qin, K.Z., Li, C., Qi, L., Su, B.X., Qu, W.J., 2011. Zircon dating, Hf–Sr–Nd–Os isotopes and PGE geochemistry of the Tianyu sulfide-bearing mafic–ultramafic intrusion in the Central Asian Orogenic Belt, NW China. Lithos 126, 84–98.
Tao, Y., Li, C., Hu, R.Z., Ripley, E.M., Du, A.D., Zhong, H., 2007. Petrogenesis of the Pt–Pd mineralized Jinbaoshan ultramafic intrusion in the Permian Emeishan Large Igneous Province, SW China. Contrib. Mineral. Petrol. 153, 321–337.
Tao, Y., Li, C., Song, X.Y., Ripley, E.M., 2008. Mineralogical, petrological, and geochemical studies of the Limahe mafic–ultramatic intrusion and associated Ni–Cu sulfide ores, SW China. Miner. Deposita 43, 849–872.
Tredoux, M., Sellschop, F.J.P., Davies, G., de Wit, M.J., 1985. The behavior of the PGE and Au during partial melting and fractional crystallization; evidence from magmas on the Kaapvaal Craton. Can. Mineral. 23, 317–318.
Wang, C.Y., Zhou, M.F., 2006. Genesis of the Permian Baimazhai magmatic Ni–Cu–(PGE) sulfide deposit, Yunnan, SW China. Miner. Deposita 41, 771–783.
Wang, C.Y., Zhou, M.F., Keays, R.R., 2006. Geochemical constraints on the origin of the Permian Baimazhai mafic–ultramafic intrusion, SW China. Contrib. Mineral. Petrol. 152, 309–321.
Wang, C.Y., Zhou, M.F., Qi, L., 2007. Permian flood basalts and mafic intrusions in the Jinping (SW China)–Song Da (northern Vietnam) district: mantle sources, crustal contamination and sulfide segregation. Chem. Geol. 243, 317–343.
Wang, C.Y., Zhou, M.F., Zhao, D.G., 2008. Fe–Ti–Cr oxides from the Permian Xinjie mafic–ultramafic layered intrusion in the Emeishan Large Igneous Province, SW China: crystallization from Fe- and Ti-rich basaltic magmas. Lithos 102, 198–217.
Xiao, L., Xu, Y.G., Mei, H.J., Zheng, Y.F., He, B., Pirajno, F., 2004a. Distinct mantle sources of low-Ti and high-Ti basalts from the western Emeishan Large Igneous Province, SW China: implications for plume–lithosphere interaction. Earth Planet. Sci. Lett. 228, 525–546.
Xiao, L., Xu, Y.G., Xu, J.F., He, B., Pirajno, F., 2004b. Chemostratigraphy of flood basalts in the Garze–Litang region and Zongza block: implications for western extension of the Emeishan Large Igneous Province, SW China. Acta Geol. Sin. 78, 61–67.
Xu, Y.G., Chung, S.L., 2001. The Emeishan Large Igneous Province: evidence for mantle plume activity and melting conditions. Geochemica 30, 1–9 (in Chinese with English abstract).
Xu, Y.G., Chung, S.L., Jahn, B.M., Wu, G.Y., 2001. Petrologic and geochemical constraints on the petrogenesis of Permian–Triassic Emeishan flood basalts in southwestern China. Lithos 58, 145–168.
Xu, J.F., Suzuki, K., Xu, Y.G., Mei, H.J., Li, J., 2007. Os, Pb, and Nd isotope geochemistry of the Permian Emeishan continental flood basalts: insights into the source of a large igneous province. Geochim. Cosmochim. Acta 71, 2104–2119.
Yao, P.H., Wang, K.N., Du, C.L., Lin, Z.T., Song, X., 1993. Records of China's Iron Ore Deposits. Metallurgical Industry Press, Beijing, pp. 638–641 (in Chinese).
Zhang, Z.C., Mao, J.W., Mahoney, J., Wang, F.S., Qu, W.J., 2005. Platinum group elements in the Emeishan Large Igneous Province, SW China: implications for mantle sources. Geochem. J. 39, 371–382.
Zhang, Z.C., Mahoney, J.J., Mao, J.W., Wang, F.S., 2006. Geochemistry of picritic and associated basalt flows of the western Emeishan flood basalt province, China. J. Petrol. 47, 1997–2019.
Zhang, Z.C., Zhi, X.C., Chen, L., Saunders, A.D., Reichow, M.K., 2008. Re–Os isotopic compositions of picrites from the Emeishan flood basalt province, China. Earth Planet. Sci. Lett. 276, 30–39.
Zhang, Z.C., Mao, J.W., Saunders, A.D., Ai, Y., Li, Y., Zhao, L., 2009. Petrogenetic modeling of three mafic–ultramafic layered intrusions in the Emeishan large igneous province, SW China, based on isotopic and bulk chemical constraints. Lithos 113, 369–392.
Zhong, H., Zhu, W.G., 2006. Geochronology of layered mafic intrusions from the Pan–Xi area in the Emeishan Large Igneous Province, SW China. Miner. Deposita 41, 599–606.
Zhong, H., Zhou, X.H., Zhou, M.F., Sun, M., Liu, B.G., 2002. Platinum-group element geochemistry of the Hongge Fe–V–Ti deposit in the Pan–Xi area, southwestern China. Miner. Deposita 37, 226–239.
Zhong, H., Yao, Y., Hu, S.F., Zhou, X.H., Liu, B.G., Sun, M., Zhou, M.F., Viljoen, M.J., 2003. Trace-element and Sr–Nd isotopic geochemistry of the PGE-bearing Hongge Layered intrusion, Southwestern China. Int. Geol. Rev. 45, 371–382.
Zhong, H., Yao, Y., Prevec, S.A., Wilson, A.H., Viljoen, M.J., Viljoen, R.P., Liu, B.-G., Luo, Y.-N., 2004. Trace-element and Sr–Nd isotopic geochemistry of the PGE-bearing Xinjie layered intrusion in SW China. Chem. Geol. 203, 237–252.
Zhong, H., Zhu, W.G., Qi, L., Zhou, M.F., Song, X.Y., Zhang, Y., 2006. Platinum-group element (PGE) geochemistry of the Emeishan basalts in the Pan–Xi area, SW China. Chin. Sci. Bull. 51, 845–854.
Zhong, H., Qi, L., Hu, R.Z., Zhou, M.F., Gou, T.Z., Zhu, W.G., Liu, B.G., Chu, Z.Y., 2011. Rhenium–osmium isotope and platinum-group elements in the Xinjie layered intrusion, SW China: implications for source mantle composition, mantle evolution, PGE fractionation and mineralization. Geochim. Cosmochim. Acta 75, 1621–1641.
Zhou, M.F., Malpas, J., Song, X.Y., Robinson, P.T., Sun, M., Kennedy, A.K., Lesher, C.M., Keays, R.R., 2002. A temporal link between the Emeishan Large Igneous Province (SW China) and the end-Guadalupian mass extinction. Earth Planet. Sci. Lett. 196, 113–122.
Zhou, M.F., Robinson, P.T., Lesher, C.M., Keays, R.R., Zhang, C.J., Malpas, J., 2005. Geochemistry, petrogenesis and metallogenesis of the Panzhihua gabbroic layered intrusion and associated Fe–Ti–V oxide deposits, Sichuan Province, SW China. J. Petrol. 46, 2253–2280.
Zhou, M.F., Ma, Y.X., Yan, D.P., Xia, X., Zhao, J.H., Sun, M., 2006. The Yanbian Terrane (Southern Sichuan Province, SW China): a Neoproterozoic arc assemblage in the western margin of the Yangtze Block. Precambrian Res. 144, 19–38.
Zhou, M.F., Arndt, N.T., Malpas, J., Wang, C.Y., Kennedy, A.K., 2008. Two magma series and associated ore deposit types in the Permian Emeishan Large Igneous Province, SW China. Lithos 103, 352–368.
Zhu, W.G., Zhong, H., Deng, H.L., Wilson, A.H., Liu, B.G., Li, C.Y., Qin, Y., 2006. SHRIMP zircon U–Pb age, geochemistry, and Nd–Sr isotopes of the Gaojiacun mafic–ultramafic intrusive complex, Southwest China. Int. Geol. Rev. 48, 650–668.
Zhu, W.G., Zhong, H., Hu, R.Z., Liu, B.G., He, D.F., Song, X.Y., Deng, H.L., 2010. Platinum-group minerals and tellurides from the PGE-bearing Xinjie layered intrusion in the Emeishan Large Igneous Province, SW China. Mineral. Petrol. 98, 167–180.